Provided for non-commercial research and education use.
Not for reproduction, distribution or commercial use.

This article was published in an Elsevier journal. The attached copy is furnished to the author for non-commercial research and education use, including for instruction at the author's institution, sharing with colleagues and providing to institution administration.

Other uses, including reproduction and distribution, or selling or licensing copies, or posting to personal, institutional or third party websites are prohibited.

In most cases authors are permitted to post their version of the article (e.g. in Word or Tex form) to their personal website or institutional repository. Authors requiring further information regarding Elsevier's archiving and manuscript policies are encouraged to visit:

http://www.elsevier.com/copyright

Author's personal copy

Available online at www.sciencedirect.com
ScienceDirect
Journal of the Mechanics and Physics of Solids
55 (2007) 2717–2734

JOURNAL OF THE MECHANICS AND PHYSICS OF SOLIDS

www.elsevier.com/locate/jmps

New phenomena concerning a screw dislocation interacting with two imperfect interfaces

X. Wang[a,b], E. Pan[a,b,*], A.K. Roy[c]

[a]*Department of Civil Engineering, University of Akron, Akron, OH 44325-3905, USA*
[b]*Department of Applied Mathematics, University of Akron, Akron, OH 44325-3905, USA*
[c]*Air Force Research Laboratory, AFRL/MLBCM, Building 654, 2941 Hobson Way, Wright-Patterson AFB, OH 45433-7750, USA*

Received 18 December 2006; received in revised form 24 March 2007; accepted 28 March 2007

Abstract

Dislocation mobility and stability in nanocrystals and electronic materials are influenced by the material composition and interface conditions. Its mobility and stability then affect the mechanical behaviors of the composites. In this paper, we first address, in detail, the problem of a screw dislocation located in an annular coating layer which is imperfectly bonded to the inner circular inhomogeneity and to the outer unbounded matrix. Both the inhomogeneity–coating interface and coating–matrix interface are modeled by a linear spring with vanishing thickness to account for the possible damage occurring on the interface. An analytic solution in series form is derived by means of complex variable method, with all the unknown constants being determined explicitly. The solution is then applied to the study of the dislocation mobility and stability due to its interaction with the two imperfect interfaces. The most interesting finding is that when the middle coating layer is more compliant than both the inner inhomogeneity and the outer unbounded matrix and when the interface rigidity parameters for the two imperfect interfaces are greater than certain values, one stable and two unstable equilibrium positions can exist for the dislocation. Furthermore, under certain conditions an equilibrium position, which can be either stable or unstable (i.e., a saddle point), can exist, which has never been observed in previous studies. Results for a screw dislocation interacting with two parallel straight imperfect interfaces are also presented as the limiting case where the radius of the inner inhomogeneity approaches infinity while the thickness of the coating layer is fixed.
© 2007 Elsevier Ltd. All rights reserved.

Keywords: Screw dislocation; Imperfect interface; Image force; Equilibrium position; Dislocation mobility and stability

*Corresponding author.
E-mail address: pan2@uakron.edu (E. Pan).

0022-5096/$ - see front matter © 2007 Elsevier Ltd. All rights reserved.
doi:10.1016/j.jmps.2007.03.017

Author's personal copy

1. Introduction

In semiconductor materials, dislocation formation and interaction can greatly influence the strain field in the material system (Freund, 2000), and thus can affect both the electronic and mechanical properties of the materials (Justo et al., 2001). However, dislocation mobility and stability are complicated phenomena, depending upon many factors, including size effects in nanocrystal case (Gryaznov et al., 1991), temperature (Abe et al., 2003), composition and interface conditions (Penn and Banfield, 1998; Hurtado and Freund, 1999). This paper concerns with the effect of composition and imperfect interface on a screw dislocation. Interfacial imperfections could be due to interdiffusion and interface vacancies (Twu and Ho, 2003), interface roughness and adhesion (Buehler et al., 2006), or simply due to the weak mechanical behavior of the interfacial zone (Kattis and Mavroyannis, 2006).

Effect of interfacial zone or imperfect interface on mechanical behavior is crucial in the design of fiber-reinforced composites (e.g., Achenbach and Zhu, 1989; Ru, 1999). Recently, the interaction of a screw dislocation with a coated circular inhomogeneity (fiber) was investigated by Xiao and Chen (2000). One interesting finding by Xiao and Chen (2000) on the equilibrium position of the image force of the dislocation is that if the coating is thin enough and if the inhomogeneity is harder while the coating is softer than the surrounding matrix, one unstable equilibrium position near the coating–matrix interface can be found. On the other hand, if the coating is thin enough and if the inhomogeneity is softer while the coating is harder than the surrounding matrix, one stable equilibrium position near the coating–matrix interface can be found. A similar problem was analyzed by Sudak (2003) where the coating layer with finite thickness was replaced by a linear-spring layer of vanishing thickness. Sudak (2003) also found that when the inhomogeneity is harder than the matrix, an unstable equilibrium position can be found. Wang and Zhong (2003) considered the interaction of a screw dislocation with a nonuniformly coated circular inhomogeneity. Their results show that two equilibrium positions of different nature, one stable and the other unstable, may coexist when the inner inhomogeneity–coating interface is nearly in contact with the outer coating–matrix interface at one point.

The above investigations show that when a screw dislocation interacts with an imperfect interface (a coating layer with finite thickness or a linear-spring model with vanishing thickness), some equilibrium positions for the dislocation near the interface can be observed. While these results based on only one imperfect interface are important to composite design, fiber-reinforced composites could contain two or more interfaces (e.g., Lafdi, 2005; Nie and Basaran, 2005; Pan and Roy, 2006), with both being imperfect. In other words, there is a need for understanding the interaction of a dislocation with two imperfect interfaces as shown in Figs. 1 and 6. In this paper, we adopt the simple but common linear-spring imperfect interface model for simulating the possible damage on the interface (for more details see Benveniste and Miloh, 1986; Achenbach and Zhu, 1989; Hashin, 1991; Ru and Schiavone, 1997; Chen, 2001; Wang and Shen, 2002; Fan and Wang, 2003; Benveniste, 2006; Sudak and Wang, 2006; Kattis and Mavroyannis, 2006). We want to understand that, if there is a screw dislocation in the intermediate coating layer, what would be the effect of the imperfect inner inhomogeneity–coating interface and the outer coating–matrix interface on its mobility and stability. If the middle coating layer is thick enough, then we can discuss the interaction of a screw dislocation with the inner imperfect

Author's personal copy

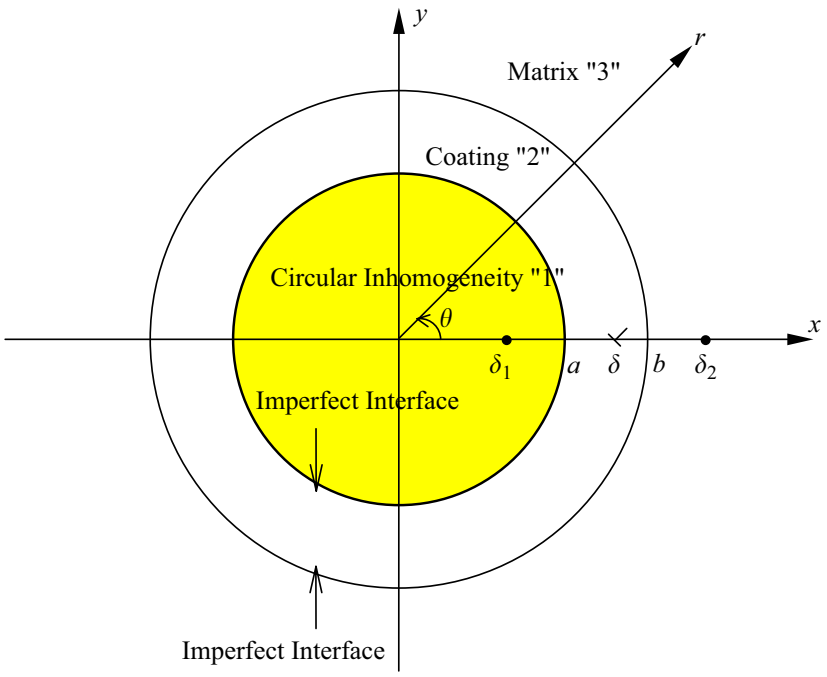

Fig. 1. A screw dislocation within an annular coating layer which is imperfectly bonded to a circular inhomogeneity and the surrounding matrix.

inhomogeneity–coating interface and with the outer imperfect coating–matrix interface separately. Under certain imperfect interface conditions, an unstable equilibrium position could be found near the imperfect inhomogeneity–coating interface (Xiao and Chen, 2000; Sudak, 2003). Similarly another unstable equilibrium position could exist near the imperfect coating–matrix interface. Since the image force on the dislocation is *continuous*, a stable equilibrium position should exist, which should be located between the two unstable equilibrium positions. This hypothesis prompts us to investigate in detail the problem of a screw dislocation lodged in an annulus coating layer which is imperfectly bonded to the inner circular inhomogeneity and to the outer unbounded matrix (Fig. 1). As shown in this paper, our study indeed confirms the co-existence of one stable and two unstable equilibrium positions for the dislocation. Our results reveal further that the situations concerning the equilibrium positions are rather complex and interesting. For example a saddle point for the equilibrium position, which can be either stable or unstable, can be also observed under certain conditions. To the best of the authors' knowledge, this important finding has never been reported in any previous literature, and could be important to our understanding of dislocation mobility and stability phenomena.

This paper is organized as follows. In Section 2 a general solution is derived for the problem of a screw dislocation located within an annular coating layer, which is imperfectly bonded to the inner circular cylindrical inhomogeneity and to the outer unbounded matrix. The linear-spring model is utilized to simulate both the inhomogeneity–coating and coating–matrix interfaces. In Section 3 the image force on the screw dislocation due to its interaction with the two imperfect interfaces are discussed in detail. In this Section we also present the results for a screw dislocation interacting with two parallel straight imperfect interfaces as a limiting case. We draw our conclusions in Section 4.

Author's personal copy

2. General solution

We first establish a Cartesian coordinate system (x, y) and a polar coordinate system (r, θ). As shown in Fig. 1, the inner circular region $r \leqslant a$ (phase "1") is the inhomogeneity with shear modulus μ_1; the intermediate annular region $a \leqslant r \leqslant b$ (phase "2") is the coating layer with shear modulus μ_2; the outer unbounded region $r \geqslant b$ (phase "3") is the matrix with shear modulus μ_3. A screw dislocation with the Burgers vector $\hat{b}$ is located at point $(\delta, 0)$, $a < \delta < b$, within the intermediate coating layer.

For the problem considered, the out-of-plane displacement w (i.e., u_z), the stress components σ_{zx}, σ_{zy} in the Cartesian coordinate system and the stress components σ_{zr}, $\sigma_{z\theta}$ in the polar coordinate system can be expressed in terms of a single analytic function $f(z)$ as

$$\begin{aligned} &w = \mathrm{Im}\{f(z)\}, \\ &\sigma_{zy} + \mathrm{i}\sigma_{zx} = \mu f'(z), \\ &\sigma_{z\theta} + \mathrm{i}\sigma_{zr} = \mu \mathrm{e}^{\mathrm{i}\theta} f'(z), \end{aligned} \tag{1}$$

where $z = x + \mathrm{i}y = r\mathrm{e}^{\mathrm{i}\theta}$ is the complex variable. In this paper, the superscripts (1), (2) and (3) will be used to denote the physical quantities (such as stress components and out-of-plane displacement) in phases 1, 2 and 3, respectively. The analytic functions defined in the three phases 1, 2 and 3 will be denoted by $f_1(z)$, $f_2(z)$ and $f_3(z)$.

To account for the possible damage occurring on the interface, we assume that both the inhomogeneity–coating interface and coating–matrix interface are imperfect and are further described by a linear spring model. In other words, the continuity condition on the inhomogeneity–coating interface $r = a$ is given by

$$\sigma_{zr}^{(1)} = \sigma_{zr}^{(2)} = k_1(w^{(2)} - w^{(1)}), \quad (r = a), \tag{2}$$

where k_1 is the spring constant of the inhomogeneity–coating interface $r = a$. It is obvious that while $k_1 = 0$ corresponds to a completely debonded interface, $k_1 \to \infty$ describes a perfectly bonded interface.

Similarly, the continuity condition on the coating–matrix interface $r = b$ is given by

$$\sigma_{zr}^{(2)} = \sigma_{zr}^{(3)} = k_2(w^{(3)} - w^{(2)}), \quad (r = b), \tag{3}$$

where k_2 is the spring constant of the coating–matrix interface $r = b$. It is apparent that while $k_2 = 0$ corresponds to a completely debonded interface, $k_2 \to \infty$ describes a perfectly bonded interface.

The continuity condition Eq. (2) on the interface $r = a$ can be equivalently expressed in terms of the two analytic functions $f_1(z)$ and $f_2(z)$ as follows:

$$\begin{aligned} &\mu_1 f_1^+(z) + \mu_1 \bar{f}_1^-\left(\frac{a^2}{z}\right) = \mu_2 f_2^-(z) + \mu_2 \bar{f}_2^+\left(\frac{a^2}{z}\right), \\ &k_1\left[f_2^-(z) - \bar{f}_2^+\left(\frac{a^2}{z}\right) - f_1^+(z) + \bar{f}_1^-\left(\frac{a^2}{z}\right)\right] = \frac{\mu_1}{a}\left[z f_1'^+(z) - \frac{a^2}{z}\bar{f}'^-_1\left(\frac{a^2}{z}\right)\right], \quad (|z| = a). \end{aligned} \tag{4}$$

Author's personal copy

Then it follows from Eq. (4) that

$$f_2(z)=\frac{\mu_1}{\mu_2}\bar{f}_1\left(\frac{a^2}{z}\right)+\frac{\hat{b}}{2\pi}\ln(z-\delta)-\frac{\hat{b}}{2\pi}\ln\left(\frac{z-\delta_1}{z}\right)+\frac{\hat{b}}{2\pi}\sum_{n=1}^{\infty}(A_n z^n-a^{2n}\bar{A}_n z^{-n}),$$

$$\bar{f}_2\left(\frac{a^2}{z}\right)=\frac{\mu_1}{\mu_2}f_1(z)-\frac{\hat{b}}{2\pi}\ln(z-\delta)+\frac{\hat{b}}{2\pi}\ln\left(\frac{z-\delta_1}{z}\right)-\frac{\hat{b}}{2\pi}\sum_{n=1}^{\infty}(A_n z^n-a^{2n}\bar{A}_n z^{-n}), \quad (5)$$

where $\delta_1=a^2/\delta<a$ is in the inhomogeneity as shown in Fig. 1, and A_n ($n=1,2,\ldots,+\infty$) are complex constants to be determined.

Substituting Eq. (5) into Eq. (4) and eliminating $f_2^-(z)$ and $\bar{f}_2^+(a^2/z)$, we arrive at

$$\chi f_1^+(z)+zf_1'^+(z)-\frac{\chi\Gamma_1\hat{b}}{2\pi}\ln(z-\delta)-\frac{\chi\Gamma_1\hat{b}}{2\pi}\sum_{n=1}^{\infty}A_n z^n$$
$$=\chi\bar{f}_1^-\left(\frac{a^2}{z}\right)+\frac{a^2}{z}\bar{f}_1'^-\left(\frac{a^2}{z}\right)-\frac{\chi\Gamma_1\hat{b}}{2\pi}\ln\left(\frac{z-\delta_1}{z}\right)-\frac{\chi\Gamma_1\hat{b}}{2\pi}\sum_{n=1}^{\infty}a^{2n}\bar{A}_n z^{-n}, \quad (|z|=a), \quad (6)$$

where the interface rigidity χ for the inner interface $r=a$ and the dimensionless constant Γ_1, which is similar to the two dimensionless Dundurs constants (Dundurs, 1967, 1970) for plane strain deformations, are defined by

$$\chi=ak_1\frac{\mu_1+\mu_2}{\mu_1\mu_2}, \quad \Gamma_1=\frac{2\mu_2}{\mu_1+\mu_2}. \quad (7)$$

It is apparent that the left-hand side of Eq. (6) is analytic within the circle $r=a$, whilst the right-hand side is analytic outside the circle $r=a$ including the point at infinity. Consequently, the continuity condition in Eq. (6) implies that the left- and right-hand sides of Eq. (6) are identically zero within the domains on both sides of the interface $r=a$. It then follows that

$$\chi f_1(z)+zf_1'(z)=\frac{\chi\Gamma_1\hat{b}}{2\pi}\left[\ln(z-\delta)+\sum_{n=1}^{\infty}A_n z^n\right], \quad (|z|\leqslant a). \quad (8)$$

Eq. (8) is a first-order inhomogeneous differential equation for $f_1(z)$ defined within the circular inhomogeneity (i.e., phase 1). Its solution can be conveniently obtained by means of the power series expansion method as

$$f_1(z)=\frac{\chi\Gamma_1\hat{b}}{2\pi}\sum_{n=1}^{\infty}\frac{A_n-n^{-1}\delta^{-n}}{\chi+n}z^n, \quad (|z|\leqslant a). \quad (9)$$

Once $f_1(z)$ has been obtained, then it follows from Eq. (5) that

$$f_2(z)=\frac{\hat{b}}{2\pi}\ln(z-\delta)-\frac{\hat{b}}{2\pi}\ln\left(\frac{z-\delta_1}{z}\right)$$
$$+\frac{\hat{b}}{2\pi}\sum_{n=1}^{\infty}\left\{A_n z^n+\frac{[\chi(1-\Gamma_1)-n]a^{2n}\bar{A}_n-\chi(2-\Gamma_1)n^{-1}\delta_1^n}{\chi+n}z^{-n}\right\},$$
$$(a\leqslant|z|\leqslant b). \quad (10)$$

Author's personal copy

Similarly the continuity condition Eq. (3) on the interface $r=b$ can be equivalently expressed in terms of the two analytic functions $f_2(z)$ and $f_3(z)$ as follows:

$$\mu_2 f_2^+(z)+\mu_2\bar{f}_2^-\left(\frac{b^2}{z}\right)=\mu_3 f_3^-(z)+\mu_3\bar{f}_3^+\left(\frac{b^2}{z}\right),$$
$$k_2\left[f_3^-(z)-\bar{f}_3^+\left(\frac{b^2}{z}\right)-f_2^+(z)+\bar{f}_2^-\left(\frac{b^2}{z}\right)\right]$$
$$=\frac{\mu_3}{b}\left[z{f'}_3^-(z)-\frac{b^2}{z}\bar{f'}_3^+\left(\frac{b^2}{z}\right)\right],\quad (|z|=b). \tag{11}$$

It follows from Eq. (11) that

$$f_2(z)=\frac{\mu_3}{\mu_2}\bar{f}_3\left(\frac{b^2}{z}\right)+\frac{\hat{b}}{2\pi}\ln(z-\delta)-\frac{\hat{b}}{2\pi}\ln(z-\delta_2)$$
$$+\frac{\mu_3}{\mu_2}\frac{\hat{b}}{2\pi}\ln z+\frac{\hat{b}}{2\pi}\sum_{n=1}^{\infty}(B_n z^n-b^{2n}\bar{B}_n z^{-n})$$
$$\bar{f}_2\left(\frac{b^2}{z}\right)=\frac{\mu_3}{\mu_2}f_3(z)-\frac{\hat{b}}{2\pi}\ln(z-\delta)+\frac{\hat{b}}{2\pi}\ln(z-\delta_2)$$
$$-\frac{\mu_3}{\mu_2}\frac{\hat{b}}{2\pi}\ln z-\frac{\hat{b}}{2\pi}\sum_{n=1}^{\infty}(B_n z^n-b^{2n}\bar{B}_n z^{-n}), \tag{12}$$

where $\delta_2=b^2/\delta>b$ is in the matrix as shown in Fig. 1, and B_n $(n=1,2,\ldots,+\infty)$ are complex constants to be determined.

Substituting Eq. (12) into Eq. (11) and eliminating $f_2^+(z)$ and $\bar{f}_2^-(b^2/z)$, we finally arrive at

$$\gamma f_3^-(z)-z{f'}_3^-(z)-\gamma\Gamma_2\frac{\hat{b}}{2\pi}\ln(z-\delta)-\gamma(1-\Gamma_2)\frac{\hat{b}}{2\pi}\ln z+\frac{\gamma\Gamma_2\hat{b}}{2\pi}\sum_{n=1}^{\infty}b^{2n}\bar{B}_n z^{-n}$$
$$=\gamma\bar{f}_3^+\left(\frac{b^2}{z}\right)-\frac{b^2}{z}\bar{f'}_3^+\left(\frac{b^2}{z}\right)-\gamma\Gamma_2\frac{\hat{b}}{2\pi}\ln(z-\delta_2)+\gamma\frac{\hat{b}}{2\pi}\ln z$$
$$+\frac{\gamma\Gamma_2\hat{b}}{2\pi}\sum_{n=1}^{\infty}B_n z^n,\quad (|z|=b), \tag{13}$$

where the interface rigidity γ for the interface $r=b$ and the dimensionless constant Γ_2 are defined by

$$\gamma=bk_2\frac{\mu_2+\mu_3}{\mu_2\mu_3},\quad \Gamma_2=\frac{2\mu_2}{\mu_2+\mu_3}. \tag{14}$$

It is apparent that the right-hand side of Eq. (13) is analytic within the circle $r=b$, whilst the left-hand side is analytic outside the circle including the point at infinity. Consequently the continuity condition in Eq. (13) implies that the left- and right-hand sides of Eq. (13) are identically zero outside and within the circle $r=b$. It then follows that

$$\gamma f_3(z)-z{f'}_3(z)=\frac{\gamma\Gamma_2\hat{b}}{2\pi}\left[\ln\left(\frac{z-\delta}{z}\right)-\sum_{n=1}^{\infty}b^{2n}\bar{B}_n z^{-n}\right]+\gamma\frac{\hat{b}}{2\pi}\ln z,\quad (|z|\geqslant b). \tag{15}$$

Author's personal copy

Eq. (15) is a first-order inhomogeneous differential equation for $f_3(z)$ defined in the unbounded matrix. Solution to this equation can also be easily obtained by means of power series expansion method as

$$f_3(z) = \frac{\hat{b}}{2\pi} \ln z - \frac{\gamma \Gamma_2 \hat{b}}{2\pi} \sum_{n=1}^{\infty} \frac{b^{2n}\bar{B}_n + n^{-1}\delta^n}{\gamma + n} z^{-n}, \quad (|z| \geqslant b). \tag{16}$$

Once $f_3(z)$ is obtained, then it follows from Eq. (12) that

$$\begin{aligned} f_2(z) = {} & \frac{\hat{b}}{2\pi} \ln(z-\delta) - \frac{\hat{b}}{2\pi} \ln(z-\delta_2) \\ & + \frac{\hat{b}}{2\pi} \sum_{n=1}^{\infty} \left\{ \frac{[\gamma(\Gamma_2 - 1) + n]B_n - \gamma(2-\Gamma_2)n^{-1}\delta_2^{-n}}{\gamma + n} z^n - b^{2n}\bar{B}_n z^{-n} \right\}, \\ & (a \leqslant |z| \leqslant b). \end{aligned} \tag{17}$$

By enforcing the continuity condition Eq. (2) on the inner interface $r = a$, we obtain the expression Eq. (10) for $f_2(z)$; by enforcing the continuity condition Eq. (3) on the outer interface $r = b$, we obtain another expression Eq. (17) for $f_2(z)$. It follows that Eqs. (17) and (10) should be the same to ensure the uniqueness of the displacement and stress fields within the coating layer. Therefore, we arrive at the following set of linear algebraic equations for the unknowns A_n, B_n $(n = 1, 2, \ldots, +\infty)$

$$\begin{aligned} & a^{2n}[\chi(1-\Gamma_1) - n]A_n + b^{2n}(\chi + n)B_n = \delta_1^n \left[n^{-1}\chi(1-\Gamma_1) - 1 \right], \\ & (\gamma + n)A_n - [\gamma(\Gamma_2 - 1) + n]B_n = \delta_2^{-n} \left[n^{-1}\gamma(\Gamma_2 - 1) + 1 \right], \quad (n = 1, 2, \ldots, +\infty). \end{aligned} \tag{18}$$

These unknowns A_n, B_n $(n = 1, 2, \ldots, +\infty)$ can be uniquely determined from Eq. (18) as

$$\begin{aligned} A_n = {} & \frac{[\gamma(1-\Gamma_2) - n]\left\{ \delta_1^n[\chi(1-\Gamma_1) - n] + b^{2n}\delta_2^{-n}(\chi + n) \right\}}{n\left\{ a^{2n}[\chi(1-\Gamma_1) - n][\gamma(1-\Gamma_2) - n] - b^{2n}(\chi + n)(\gamma + n) \right\}}, \\ B_n = {} & \frac{[\chi(\Gamma_1 - 1) + n]\left\{ \delta_1^n(\gamma + n) + \delta_2^{-n}a^{2n}[\gamma(1-\Gamma_2) - n] \right\}}{n\left\{ a^{2n}[\chi(1-\Gamma_1) - n][\gamma(1-\Gamma_2) - n] - b^{2n}(\chi + n)(\gamma + n) \right\}}, \\ & (n = 1, 2, \ldots, +\infty), \end{aligned} \tag{19}$$

which indicates that A_n, B_n $(n = 1, 2, \ldots, +\infty)$ are in fact real values.

In summary, the three analytic functions ($f_1(z)$in the circular inhomogeneity $|z| \leqslant a$, $f_2(z)$ in the coating $a \leqslant |z| \leqslant b$, and $f_3(z)$ in the unbounded matrix $|z| \geqslant b$) have now been totally determined. With these functions, the displacement and stress fields induced by the screw dislocation can be obtained from Eq. (1) for the three phases. For example the stress component σ_{zy} on the real axis within the coating layer is obtained as follows

$$\begin{aligned} \sigma_{zy} = {} & \frac{\mu_2 \hat{b}}{2\pi} \frac{1}{x-\delta} - \frac{\mu_2 \hat{b}}{2\pi} \frac{\delta_1}{x(x-\delta_1)} \\ & + \frac{\mu_2 \hat{b}}{2\pi} \sum_{n=1}^{\infty} \left\{ nA_n x^{n-1} + \frac{n[\chi(\Gamma_1 - 1) + n]a^{2n}A_n + \chi(2-\Gamma_1)\delta_1^n}{\chi + n} x^{-n-1} \right\}, \\ & (a \leqslant x \leqslant b), \end{aligned} \tag{20}$$

which is essential when forming the singular integral equation for a radial crack in the coating layer interacting with two imperfect interfaces.

Author's personal copy

We remark that the solution developed can be easily extended to the remote uniform shearing case (i.e., under σ_{zx}^{∞} and σ_{zy}^{∞}). Actually, for this case, the three analytic functions $f_1(z)$, $f_2(z)$ and $f_3(z)$ can be similarly derived as follows:

$$f_1(z)=\frac{R\chi\gamma\Gamma_1(2-\Gamma_2)(\sigma_{zy}^{\infty}+\mathrm{i}\sigma_{zx}^{\infty})}{\mu_3\{R(\chi+1)(\gamma+1)-[\chi(\Gamma_1-1)+1][\gamma(\Gamma_2-1)+1]\}}z,\quad (|z|\leqslant a), \tag{21}$$

$$f_2(z)=\frac{\gamma(2-\Gamma_2)\left\{R(\chi+1)(\sigma_{zy}^{\infty}+\mathrm{i}\sigma_{zx}^{\infty})z-b^2[\chi(\Gamma_1-1)+1](\sigma_{zy}^{\infty}-\mathrm{i}\sigma_{zx}^{\infty})z^{-1}\right\}}{\mu_3\{R(\chi+1)(\gamma+1)-[\chi(\Gamma_1-1)+1][\gamma(\Gamma_2-1)+1]\}},\quad (a\leqslant|z|\leqslant b), \tag{22}$$

$$f_3(z)=\frac{\sigma_{zy}^{\infty}+\mathrm{i}\sigma_{zx}^{\infty}}{\mu_3}z+\frac{R(\chi+1)[\gamma(\Gamma_2-1)-1]-(\gamma-1)[\chi(\Gamma_1-1)+1]}{R(\chi+1)(\gamma+1)-[\chi(\Gamma_1-1)+1][\gamma(\Gamma_2-1)+1]}\times\frac{(\sigma_{zy}^{\infty}-\mathrm{i}\sigma_{zx}^{\infty})}{\mu_3}b^2z^{-1},\quad (|z|\geqslant b), \tag{23}$$

where

$$R=\left(\frac{b}{a}\right)^2. \tag{24}$$

It is interesting that if the three-phase composite is only subjected to the remote uniform loading, the stress field inside the circular inhomogeneity is still *uniform* and is explicitly given by

$$\sigma_{zy}+\mathrm{i}\sigma_{zx}=\frac{R\chi\gamma\Gamma_2(2-\Gamma_1)(\sigma_{zy}^{\infty}+\mathrm{i}\sigma_{zx}^{\infty})}{R(\chi+1)(\gamma+1)-[\chi(\Gamma_1-1)+1][\gamma(\Gamma_2-1)+1]},\quad (|z|\leqslant a). \tag{25}$$

Following the approach of Gong and Meguid (1992), the change of the elastic energy ΔW in the body due to the introduction of the coated circular inhomogeneity can be evaluated as

$$\Delta W=\frac{\pi b^2}{\mu_3}\frac{(\gamma-1)[\chi(\Gamma_1-1)+1]-R(\chi+1)[\gamma(\Gamma_2-1)-1]}{R(\chi+1)(\gamma+1)-[\chi(\Gamma_1-1)+1][\gamma(\Gamma_2-1)+1]}\left[(\sigma_{zy}^{\infty})^2+(\sigma_{zx}^{\infty})^2\right]. \tag{26}$$

It follows that if the inhomogeneity and coating layer are of the same material, i.e., $\Gamma_1=1$, and the two interfaces are perfect, i.e., $\chi,\ \gamma\to\infty$, then Eq. (26) reduces to

$$\Delta W=\frac{\pi b^2}{\mu_3}(1-\Gamma_2)\left[(\sigma_{zy}^{\infty})^2+(\sigma_{zx}^{\infty})^2\right], \tag{27}$$

which is just the result derived by Gong and Meguid (1992) for a perfectly bonded circular inhomogeneity.

The coated inhomogeneity is termed stealth if the uniform stress field in the matrix is not disturbed by the introduction of the coated inhomogeneity (Honein et al., 1994). It follows from Eq. (23) that the coated inhomogeneity will be stealth if the following condition is satisfied

$$R=\left(\frac{b}{a}\right)^2=\frac{(\gamma-1)[\chi(\Gamma_1-1)+1]}{(\chi+1)[\gamma(\Gamma_2-1)-1]}>1. \tag{28}$$

Author's personal copy

It is obvious that if the two interfaces are perfect, i.e., $\chi, \gamma \to \infty$, then the above condition becomes

$$R = \left(\frac{b}{a}\right)^2 = \frac{\Gamma_1 - 1}{\Gamma_2 - 1} > 1, \tag{29}$$

which is just the result derived by Honein et al. (1994). It follows from Eqs. (26) and (28) that if the coated inhomogeneity is stealth, then it will not cause any change of elastic energy, i.e., $\Delta W = 0$.

We finally remark that Eqs. (21)–(23) for the three analytic functions $f_i(z)$ $(i = 1, 2, 3)$ are very useful in predicting the effective shear modulus of the fiber-reinforced composite (Chen and Chiang, 1997; Pan and Roy, 2006). This will be pursued as a separate endeavor.

3. Image force on the dislocation

3.1. Image force on the screw dislocation interacting with two concentric circular imperfect interfaces

Here we are interested in the mobility and stability of the screw dislocation due to its interaction with the two imperfect interfaces $r = a$ and b. Particularly we will concentrate on the existence of the equilibrium position for the dislocation. By using the Peach–Koehler formula (Hirth and Lothe, 1982), the image force acting on the dislocation due to its interaction with the two imperfectly bonded interfaces can be derived to be

$$\tilde{F}_x = \sum_{n=1}^{\infty} \frac{\tilde{\delta}^{-2n-1} R^n(\gamma + n)[\chi(\Gamma_1 - 1) + n] - \tilde{\delta}^{2n-1}(\chi + n)[\gamma(\Gamma_2 - 1) + n]}{[\chi(\Gamma_1 - 1) + n][\gamma(\Gamma_2 - 1) + n] - R^n(\chi + n)(\gamma + n)}, \tag{30}$$

where R is defined by Eq. (24), and

$$\tilde{F}_x = \frac{2\pi a}{\mu_2 \hat{b}^2} F_x, \quad \tilde{\delta} = \frac{\delta}{a}, \tag{31}$$

with F_x being the x-component of the image force (the y-component of the image force on the dislocation is zero). It is observed from Eq. (30) that the value of $\tilde{F}_x$ depends on the two dimensionless parameters Γ_1 and Γ_2 (more precisely on the two mismatch parameters $\Gamma_1 - 1$ and $\Gamma_2 - 1$), the two interface rigidity parameters χ and γ, and the two geometric parameters $\tilde{\delta}$ and R. Based on their different combinations, we consider the following special cases.

(i) When $\Gamma_1 = \Gamma_2 = \Gamma$ and $\chi = \gamma = \lambda$, Eq. (30) reduces to

$$\tilde{F}_x = \sum_{n=1}^{\infty} \frac{(\lambda + n)[\lambda(\Gamma - 1) + n](\tilde{\delta}^{-2n-1} R^n - \tilde{\delta}^{2n-1})}{[\lambda(\Gamma - 1) + n]^2 - R^n(\lambda + n)^2}. \tag{32}$$

It is found from the above expression that $\delta = \sqrt{ab}$ is always an equilibrium position, i.e., $\tilde{F}_x = 0$ when $\delta = \sqrt{ab}$. In other words if $\Gamma_1 = \Gamma_2 = \Gamma$ and $\chi = \gamma = \lambda$, the equilibrium position $\delta = \sqrt{ab}$ is independent of Γ and λ.

(ii) When the coating layer and matrix are of the same material, and the coating–matrix interface is a perfect one, i.e., $\Gamma_2 = 1$ and $\gamma \to \infty$, then Eq. (30)

Author's personal copy

reduces to

$$\tilde{F}_x = -\sum_{n=1}^{\infty} \frac{\chi(\Gamma_1 - 1) + n}{\tilde{\delta}^{2n+1}(\chi + n)}, \tag{33}$$

which is just the result derived by Sudak (2003) for a screw dislocation located in the matrix interacting with an imperfectly bonded circular inhomogeneity.

(iii) When the inhomogeneity and coating layer are of the same material, and the inhomogeneity–coating interface is a perfect one, i.e., $\Gamma_1 = 1$ and $\chi \to \infty$, then Eq. (30) reduces to

$$\tilde{F}_x = \sum_{n=1}^{\infty} \frac{\tilde{\delta}^{2n-1}[\gamma(\Gamma_2 - 1) + n]}{R^n(\gamma + n)}, \tag{34}$$

which is the result for a screw dislocation inside an imperfectly bonded inhomogeneity.

(iv) When both the inhomogeneity–coating and coating–matrix interfaces are completely debonded, i.e., χ, $\gamma \to 0$, then Eq. (30) reduces to

$$\tilde{F}_x = \sum_{n=1}^{\infty} \frac{\tilde{\delta}^{-2n-1}R^n - \tilde{\delta}^{2n-1}}{1 - R^n}, \tag{35}$$

which is the image force on a screw dislocation in an annular ring $a \leqslant r \leqslant b$ whose two surfaces $r = a$ and b are traction-free.

(v) When both the inhomogeneity–coating and coating–matrix interfaces are perfect, i.e., χ, $\gamma \to \infty$, then Eq. (30) reduces to

$$\tilde{F}_x = \sum_{n=1}^{\infty} \frac{\tilde{\delta}^{-2n-1}R^n(\Gamma_1 - 1) - \tilde{\delta}^{2n-1}(\Gamma_2 - 1)}{(\Gamma_1 - 1)(\Gamma_2 - 1) - R^n}, \tag{36}$$

which will reduce to Eq. (35) by letting μ_1, $\mu_3 \to 0$ or equivalently $\Gamma_1 = \Gamma_2 = 2$.

(vi) It can be deduced from Eq. (30) that for fixed values a and b, if $\delta = \delta_c$ is an equilibrium position for a set of four parameters $\Gamma_1 = \Gamma_{1c}$, $\Gamma_2 = \Gamma_{2c}$, $\chi = \chi_c$ and $\gamma = \gamma_c$, then $\delta = (ab/\delta_c)$ is also an equilibrium position for another set of four parameters $\Gamma_1 = \Gamma_{2c}$, $\Gamma_2 = \Gamma_{1c}$, $\chi = \gamma_c$ and $\gamma = \chi_c$.

In the following we present some numerical examples based on our solutions to investigate the dependence of the equilibrium position for the dislocation on the involved parameters. In our numerical calculation we truncate the series in Eq. (30) at $n = 300$ in order to obtain the result with a relative error less than 0.01%.

First we show in Fig. 2 the variation of the image force $\tilde{F}_x$ on the dislocation within the coating layer as a function of $\tilde{\delta}$ for different values of interface rigidity $\lambda = \chi = \gamma$ with $\Gamma_1 = \Gamma_2 = 1/3$ $(\mu_1 = \mu_3 = 5\mu_2)$ and $R = 2.25$ $(b = 1.5a)$. In this configuration, the inhomogeneity and matrix are both stiffer than the coating. It is observed from Fig. 2 that when $\lambda \leqslant 6.14$, there is one common *unstable* equilibrium position $\delta = \sqrt{ab} \approx 1.22a$ for the dislocation. When $\lambda > 6.14$, however, there exist three equilibrium positions for the dislocation: two unstable near the two interfaces $r = a$, b and one *stable* at $\delta = \sqrt{ab} \approx 1.22a$. It is verified that, independent of λ, $\delta = \sqrt{ab} \approx 1.22a$ is always an equilibrium position as predicted above. However, the nature of this equilibrium position is determined by λ (i.e., whether λ is greater or smaller than the critical $\lambda_c = 6.14$). In fact

Author's personal copy

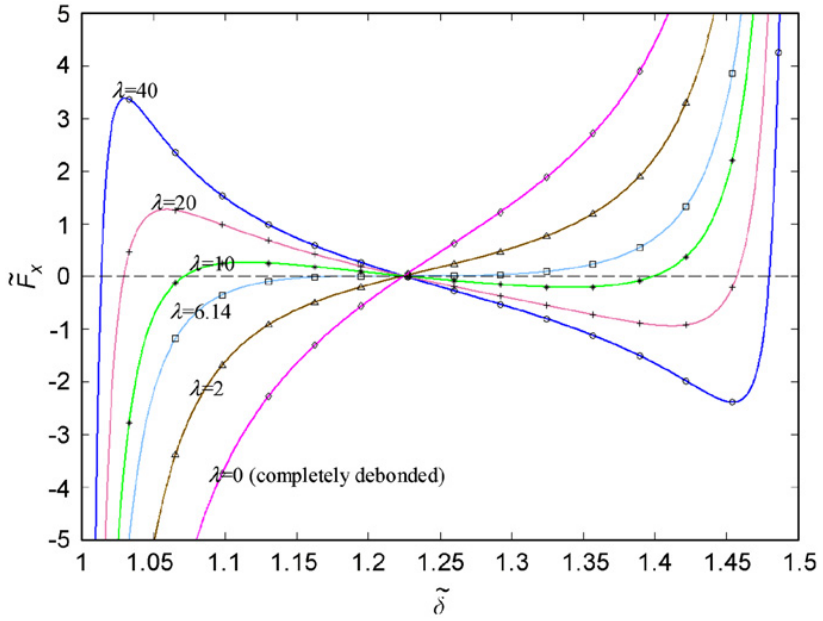

Fig. 2. Variation of the image force $\tilde{F}_x$ on the dislocation within the annular coating layer as a function of $\tilde{\delta}$ for different interface rigidity λ ($\lambda = \chi = \gamma$) with $\Gamma_1 = \Gamma_2 = 1/3$ ($\mu_1 = \mu_3 = 5\mu_2$) and $R = 2.25$ ($b = 1.5a$).

Table 1
Critical value λ_c vs. dimensionless constant Γ (from 0 to 1) with $R = 2.25$

Γ	0	0.1	0.2	1/3	0.4	0.5	0.6	0.7	0.8	0.9	1
λ_c	3.85	4.35	4.99	6.14	6.93	8.50	10.8	13.4	23.1	47.8	∞

the critical value λ_c is dependent on $\Gamma_1 = \Gamma_2 = \Gamma$, as listed in Table 1 for Γ varying from zero to 1 with fixed $R = 2.25$. It's found from Table 1 that λ_c is an increasing function of Γ and approaches infinity when $\Gamma = 1$.

Fig. 3 then shows the variation of the image force $\tilde{F}_x$ on the dislocation within the coating layer as a function of $\tilde{\delta}$, for different values of Γ_2 with $\Gamma_1 = 1/3$ ($\mu_1 = 5\mu_2$) in Fig. 3a, and for different values of Γ_1 with $\Gamma_2 = 1/3$ ($\mu_3 = 5\mu_2$) in Fig. 3b. Other fixed parameters are $\chi = \gamma = 40$ and $R = 2.25$ ($b = 1.5a$). It's observed from Fig. 3a that when $\Gamma_2 < 0.72108$ there are three equilibrium positions for the dislocation: two are unstable near the two interfaces and one is stable between the unstable ones. When $\Gamma_2 = 0.72108$ there are only two equilibrium positions at $\delta = 1.013a$ and $1.396a$. The equilibrium position $\delta = 1.013a$ is an unstable one whilst $\delta = 1.396a$ is a saddle point (i.e., if there is a small perturbation from this equilibrium position, the image force on the dislocation is always *positive*). When $\Gamma_2 > 0.72108$ there is only one unstable equilibrium position $\delta \approx 1.01a$, which is very close to the inner interface $r = a$. Similarly, it's found from Fig. 3b that when $\Gamma_1 < 0.72108$ there are three equilibrium positions for the dislocation: two are unstable near the two interfaces and one is stable between the unstable ones. When $\Gamma_1 = 0.72108$ there are two equilibrium positions $\delta = 1.074a$ and $1.480a$. While $\delta = 1.480a$ is an unstable one, $\delta = 1.074a$ is a saddle point (i.e., if there is a small perturbation from this equilibrium position, the image force on the dislocation is always *negative*). When $\Gamma_1 > 0.72108$ there is only one unstable equilibrium position $\delta \approx 1.48a$ which is very close to the outer interface

Author's personal copy

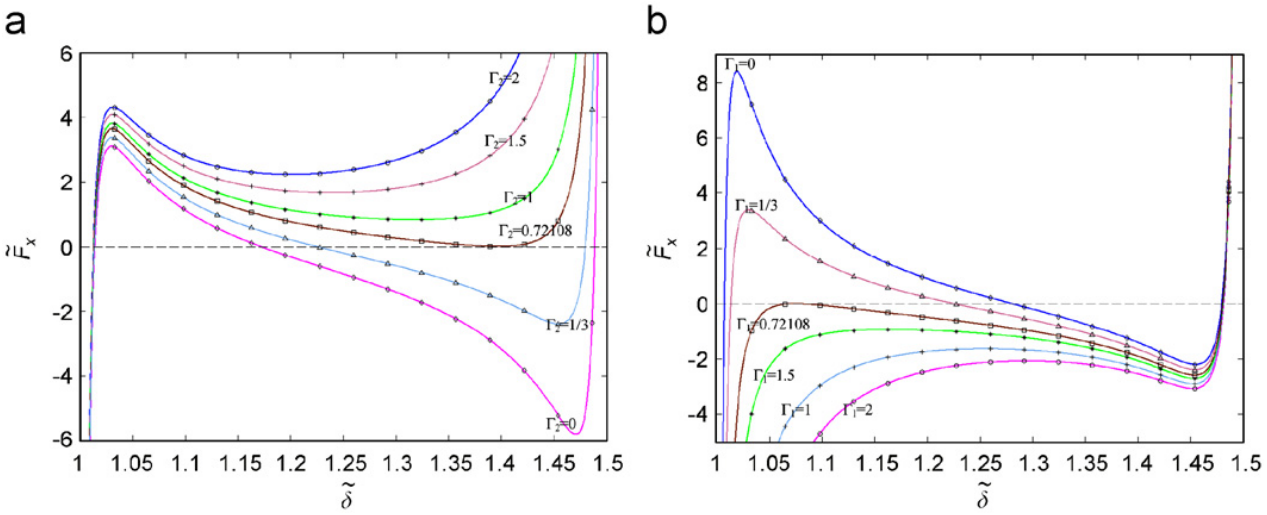

Fig. 3. Variation of the image force $\tilde{F}_x$ on the dislocation within the annular coating layer as a function of $\tilde{\delta}$ for fixed parameters $\chi = \gamma = 40$ and $R = 2.25$ ($b = 1.5a$). Results for different Γ_2 with fixed $\Gamma_1 = 1/3$ ($\mu_1 = 5\mu_2$) in (a), and for different Γ_1 with fixed $\Gamma_2 = 1/3$ ($\mu_3 = 5\mu_2$) in (b).

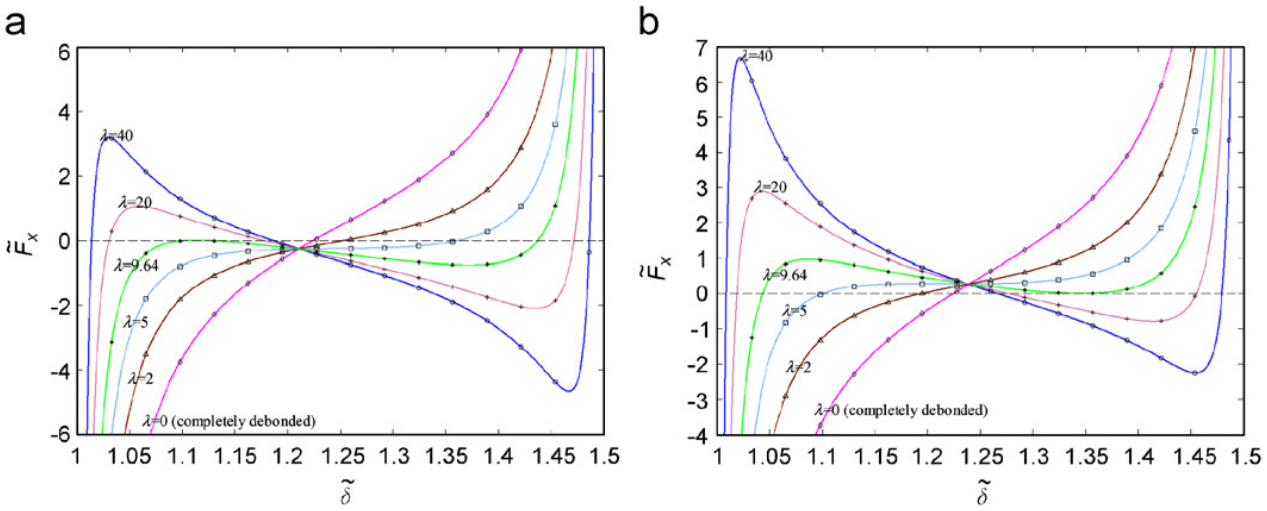

Fig. 4. Variation of the image force $\tilde{F}_x$ on the dislocation within the annular coating layer as a function of $\tilde{\delta}$ for different interface rigidity λ ($\lambda = \chi = \gamma$) and fixed $R = 2.25$ ($b = 1.5a$). Results for $\Gamma_1 = 1/3$, $\Gamma_2 = 0.1$ ($\mu_1 = 5\mu_2$, $\mu_3 = 19\mu_2$) in (a), and for $\Gamma_1 = 0.1$, $\Gamma_2 = 1/3$ ($\mu_1 = 19\mu_2$, $\mu_3 = 5\mu_2$) in (b).

$r = b$. The results shown in Figs. 3a and b are in agreement with the special feature (v) of the equilibrium position for the image force on the dislocation as discussed above. In addition it should be mentioned that the new kind of equilibrium position for the dislocation, namely the saddle point, has never been reported in any open literature.

Fig. 4 demonstrates the variation of the image force $\tilde{F}_x$ on the dislocation within the coating layer as a function of $\tilde{\delta}$ for different values of interface rigidity $\lambda = \chi = \gamma$, with $\Gamma_1 = 1/3$, $\Gamma_2 = 0.1$ ($\mu_1 = 5\mu_2$, $\mu_3 = 19\mu_2$) in Fig. 4a, and $\Gamma_1 = 0.1$, $\Gamma_2 = 1/3$ ($\mu_1 = 19\mu_2$, $\mu_3 = 5\mu_2$) in Fig. 4b. The other fixed parameter is $R = 2.25$ ($b = 1.5a$). It is noted that for the results in Fig. 4a, the matrix is the hardest, the coating layer is the softest, whilst the stiffness of the inhomogeneity is between them. For the results in Fig. 4b, on the other hand, the inhomogeneity is the hardest, the coating is the softest, whilst the stiffness of the

Author's personal copy

matrix is between them. It is observed from Fig. 4a that the curves for different values of the interface rigidity all pass through one common point below the zero-force axis. When $\lambda > 9.64$ there are three equilibrium positions for the dislocation: two unstable and one stable. When $\lambda > 9.64$ there are two equilibrium positions $\delta = 1.114a$ and $1.438a$. The equilibrium position $\delta = 1.438a$ is an unstable one whilst $\delta = 1.114a$ is a saddle point. When $\lambda < 9.64$ there is only one unstable equilibrium position. On the other hand, it is observed from Fig. 4b that the curves for different values of the interface rigidity also pass through one common point but above the zero-force axis. Similarly, when $\lambda > 9.64$ there are three equilibrium positions for the dislocation: two unstable and one stable. When $\lambda = 9.64$ there are two equilibrium positions at $\delta = 1.043a$ and $1.347a$. The equilibrium position $\delta = 1.043a$ is an unstable one whilst $\delta = 1.347a$ is a saddle point. When $\lambda < 9.64$ there is only one unstable equilibrium position. Again, the results in Figs. 4a and b are also in agreement with the special feature (v) as discussed above.

As we have demonstrated in Figs. 3 and 4 that a special new kind of equilibrium position, which is either stable or unstable (i.e., a saddle point), can be observed for certain combinations of the two dimensionless constants Γ_1, Γ_2 and the two interface rigidity parameters χ, γ. In order to understand more clearly this new phenomenon, we plot in Fig. 5 the phase diagrams for the equilibrium position for different combinations of $\Gamma_1 = \Gamma_{1c}$, $\Gamma_2 = \Gamma_{2c}$ with $R = 2.25$. While Fig. 5a is for $\chi = \gamma = \lambda = \lambda_c$, Fig. 5b is for the unequal interface rigidity case $\chi = 4\gamma$. It is important that from Fig. 5a we can easily determine the stable and unstable feature of the equilibrium positions for a fixed value of $\lambda = \lambda_c$:

(1) if the pair (Γ_1, Γ_2) lies within the closed curve formed by $(\Gamma_{1c}, \Gamma_{2c})$, the Γ_1-axis and the Γ_2-axis, there are three equilibrium positions for the dislocation: two unstable and one stable with the latter being between the two unstable ones;
(2) if the pair (Γ_1, Γ_2) lies outside the closed curve, there is only one unstable equilibrium position for the dislocation;

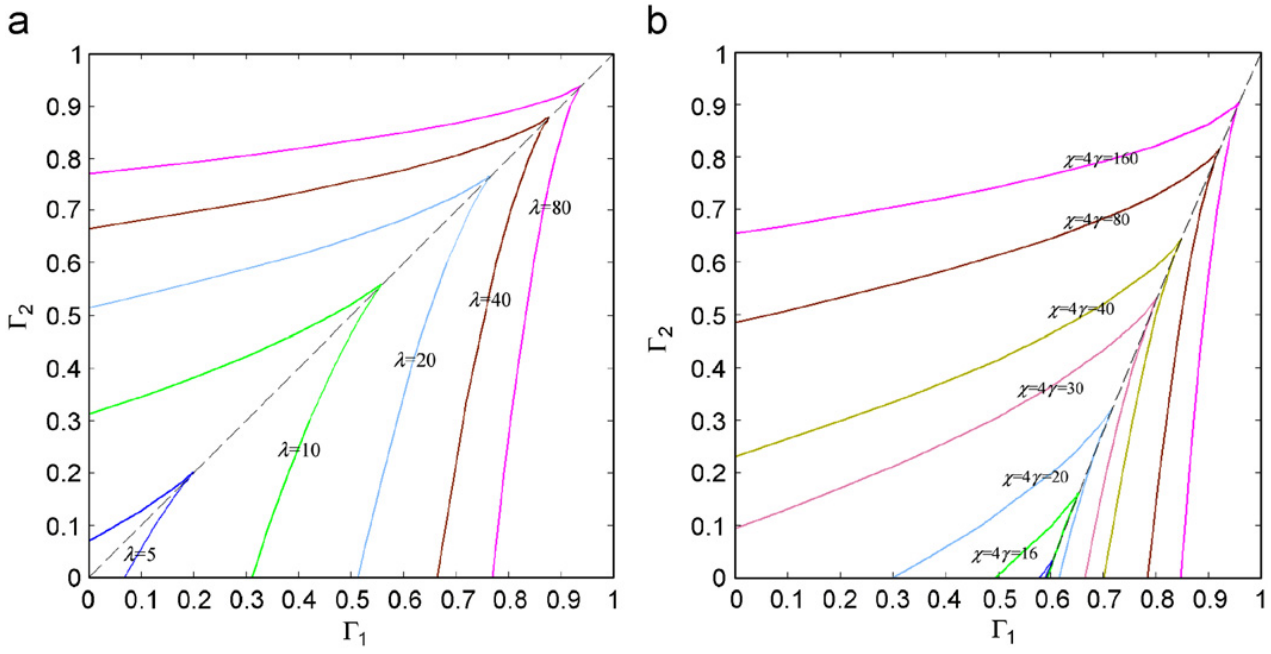

Fig. 5. Phase diagram of equilibrium positions for possible combinations of Γ_1 and Γ_2 with $R = 2.25$ ($b = 1.5a$). $\lambda = \chi = \gamma$ in (a), and $\chi = 4\gamma$ in (b).

Author's personal copy

(3) if the pair (Γ_1, Γ_2) just lies on the curve formed by (Γ_{1c}, Γ_{2c}), there are two equilibrium positions for the dislocation: one unstable and one saddle point. More precisely if (Γ_1, Γ_2) lies above the diagonal straight dash line, the unstable equilibrium position is on the left-hand side of the other equilibrium position; if (Γ_1, Γ_2) lies below the dash line, the unstable equilibrium position is on the right-hand side of the other equilibrium position; if (Γ_1, Γ_2) also lies on the dash line, there is only one unstable equilibrium position (in this special case the unstable equilibrium position and the saddle point converge to one single unstable equilibrium position).

It should be pointed out that the curves in Fig. 5a will shrink to the origin $\Gamma_1 = 0$, $\Gamma_2 = 0$ when $\lambda = 3.85$ (see Table 1). In other words if $\lambda \leqslant 3.85$, there is only one unstable equilibrium position for the dislocation independent of the dimensionless constants Γ_1 and Γ_2.

As for Fig. 5b, since an unequal interface rigidity parameter $\chi = 4\gamma$ is used, the dash line in Fig. 5b is not straight and does not pass through the origin. The curves in Fig. 5b will finally shrink to the point $\Gamma_1 = 0.59$, $\Gamma_2 = 0$ when $\chi = 4\gamma = 13.04$. The overall trend for the phase diagram in Fig. 5b is similar to that in Fig. 5a. It can be also found from Figs. 5a and 5b that the sufficient and necessary conditions for the existence of three equilibrium positions for the dislocation within the intermediate coating layer is that the intermediate coating layer should be softer than both the inhomogeneity and the matrix, i.e., Γ_1, $\Gamma_2 < 1$, and the interface rigidity parameters must be greater than certain values. If the two interface rigidity parameters are lower than certain values (e.g., $\chi = \gamma \leqslant 3.85$ and $\chi = 4\gamma \leqslant 13.04$ for $R = 2.25$), there will be only one unstable equilibrium position for the dislocation no matter what values of Γ_1 and Γ_2 are taken.

3.2. *Image force on the screw dislocation interacting with two parallel straight imperfect interfaces*

If we let the inhomogeneity radius a approach infinity and keep the thickness $h = b - a$ fixed, then our results can be used to investigate the interaction of a screw dislocation with two parallel straight imperfect interfaces, as illustrated in Fig. 6. In Fig. 6 a new coordinate system (x_1, y) is established by translating the origin of the original coordinate system (x, y) to the right intersection point between the inner circle and the horizontal axis, i.e., $x_1 = x - a$. As a result the screw dislocation in the new coordinate system is located at $x_1 = \delta - a$ and $y = 0$.

For the case of two straight interfaces, we redefine the two interface rigidity parameters χ and γ as

$$\chi = hk_1 \frac{\mu_1 + \mu_2}{\mu_1 \mu_2}, \quad \gamma = hk_2 \frac{\mu_2 + \mu_3}{\mu_2 \mu_3}. \tag{37}$$

We also redefine the normalized image force on the dislocation $\tilde{F}_x$ and the dimensionless dislocation position $\tilde{\delta}$ as

$$\tilde{F}_x = \frac{2\pi h}{\mu_2 b^2} F_x, \quad \tilde{\delta} = \frac{\delta - a}{h}. \tag{38}$$

Author's personal copy

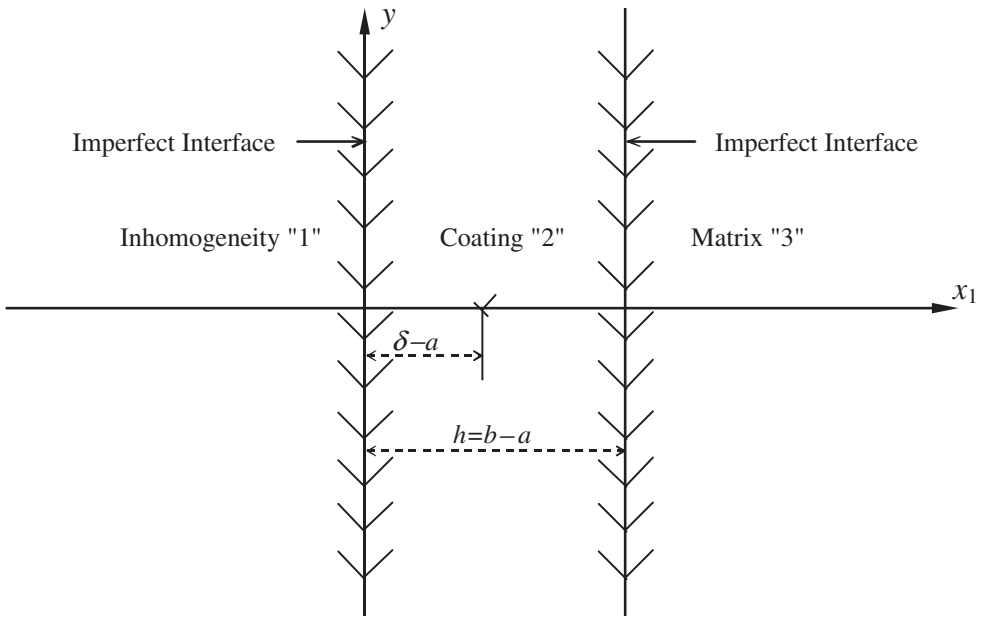

Fig. 6. A screw dislocation within a coating layer interacting with two parallel straight imperfect interfaces.

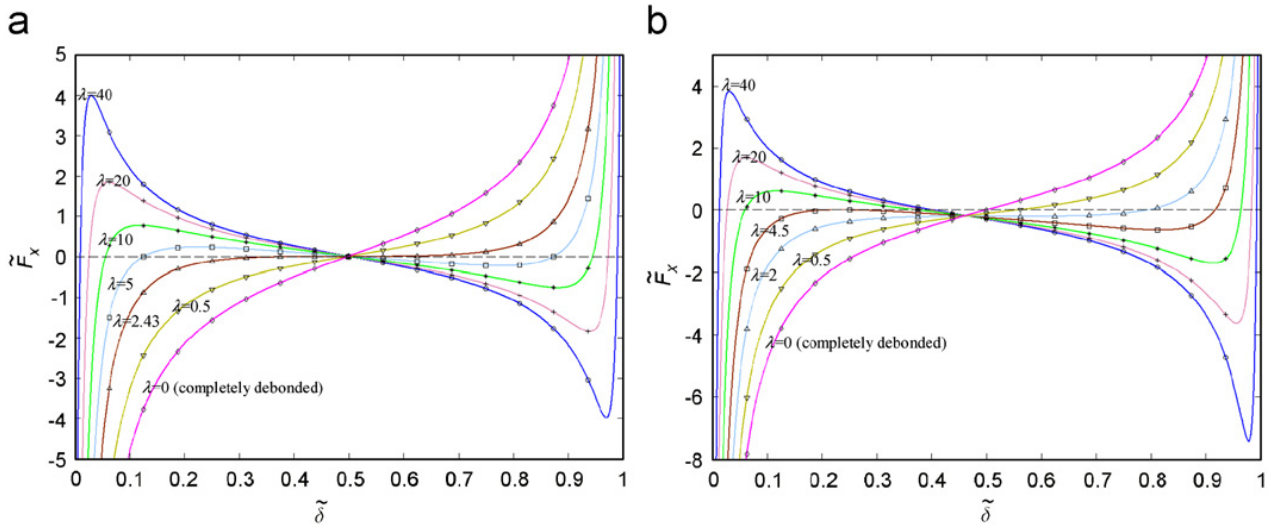

Fig. 7. Variation of the image force $\tilde{F}_x$ on the dislocation within the coating layer as a function of $\tilde{\delta}$ for different interface rigidity λ ($\lambda=\chi=\gamma$). Results for $\Gamma_1=\Gamma_2=1/3$ ($\mu_1=\mu_3=5\mu_2$) in (a), and $\Gamma_1=1/3$, $\Gamma_2=0.1$ ($\mu_1=5\mu_2$, $\mu_3=19\mu_2$) in (b).

In the following we present the results for a screw dislocation interacting with two parallel straight imperfect interfaces. In our calculation for this case, we set $a=200h$ with the series in Eq. (30) being truncated at $n=2000$ for a relative error less than 0.01%.

Fig. 7 demonstrates the variation of the image force $\tilde{F}_x$ on the dislocation as a function of $\tilde{\delta}$ for different values of interface rigidity $\lambda=\chi=\gamma$, with $\Gamma_1=\Gamma_2=1/3$ ($\mu_1=\mu_3=5\mu_2$) in Fig. 7a and $\Gamma_1=1/3$, $\Gamma_2=0.1$ ($\mu_1=5\mu_2$, $\mu_3=19\mu_2$) in Fig. 7b. It's observed from Fig. 7a that the image force for fixed λ is anti-symmetric with respect to the midpoint $\tilde{\delta}=\frac{1}{2}$, which is always an equilibrium position. This is expected since the shear moduli of the inhomogeneity "1" and the matrix "3" are the same, and the two interface rigidity parameters χ and γ are also the same. Furthermore, it is noted that (Fig. 7a) when $\lambda\leqslant 2.43$

Author's personal copy

Table 2
Critical value λ_c vs. dimensionless constant Γ (from 0 to 1)

Γ	0	0.1	0.2	1/3	0.4	0.5	0.6	0.7	0.8	0.9	1
λ_c	1.44	1.68	1.95	2.43	2.74	3.39	4.35	5.98	9.28	19.2	∞

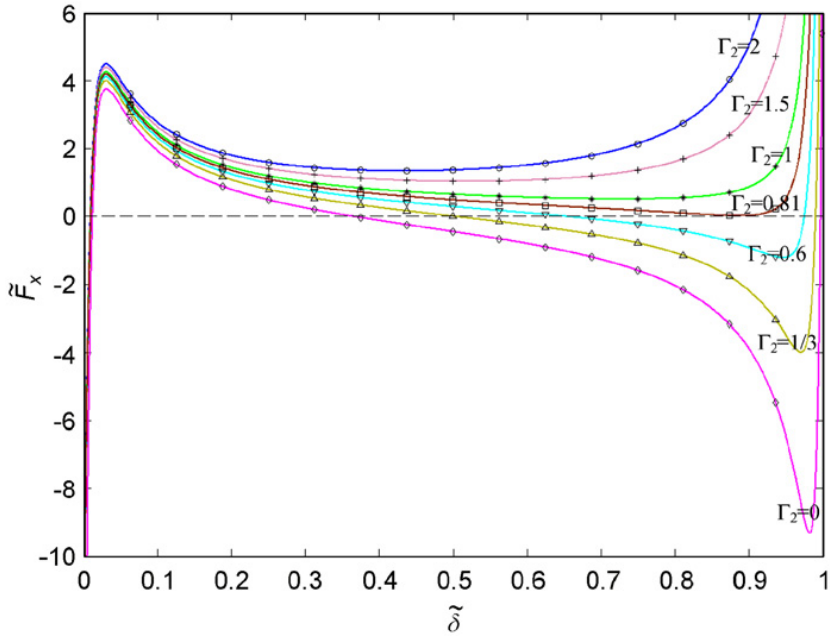

Fig. 8. Variation of the image force $\tilde{F}_x$ on the dislocation within the coating layer as a function of $\tilde{\delta}$ for different Γ_2 with $\Gamma_1 = 1/3$ ($\mu_1 = 5\mu_2$) and $\chi = \gamma = 40$.

there is only one unstable equilibrium position at the midpoint. When $\lambda > 2.43$, however, there are three equilibrium positions: two unstable ones close to the two imperfect interfaces, and one stable at the midpoint. The nature of the equilibrium position at the midpoint depends on the critical value λ_c for $\Gamma_1 = \Gamma_2 = \Gamma$. Table 2 lists the values of λ_c when Γ is increased from zero to 1. Similar to the discussion for the annulus coating case, λ_c is an increasing function of Γ and approaches infinity when $\Gamma = 1$. As for Fig. 7b, it is observed that the image forces for different values of the interface rigidity all pass through one common point below the zero-force axis, which is similar to Fig. 4a: (1) when $\lambda < 4.5$, there is only one unstable equilibrium position; (2) when $\lambda = 4.5$, there are two equilibrium positions at $\tilde{\delta} = 0.232$ and 0.916. While $\tilde{\delta} = 0.916$ is an unstable one, $\tilde{\delta} = 0.232$ is a saddle point; (3) when $\lambda > 4.5$, there are two unstable and one stable equilibrium positions.

Finally, Fig. 8 shows the variation of the image force $\tilde{F}_x$ on the dislocation as a function of $\tilde{\delta}$ for different values of Γ_2 with $\Gamma_1 = 1/3$ ($\mu_1 = 5\mu_2$) and $\chi = \gamma = 40$. It is found that Fig. 8 is similar to Fig. 3a: (1) when $\Gamma_2 < 0.81$ there exist three equilibrium positions for the screw dislocation: two unstable near the two interfaces and one stable between the two unstable ones; (2) when $\Gamma_2 = 0.81$ there are two equilibrium positions at $\tilde{\delta} = 0.0096$ and 0.886. While $\tilde{\delta} = 0.0096$ is an unstable one, $\tilde{\delta} = 0.886$ is a saddle point; (3) when $\Gamma_2 > 0.81$ there exists only one unstable equilibrium position very close to the inhomogeneity–coating interface.

Author's personal copy

4. Concluding remarks

The problem of a screw dislocation interacting with two concentric circular imperfect interfaces (or with two parallel straight imperfect interfaces in the limiting case) is addressed in detail, with an emphasis on the dislocation mobility and stability phenomena. Our results show that when the inhomogeneity–coating and coating–matrix interfaces are imperfect, there are three types of equilibrium positions for the image force applied on the dislocation within the coating layer: (1) one single unstable equilibrium position; (2) two equilibrium positions: one is unstable and the other one is either stable or unstable (i.e., the saddle point); (3) three equilibrium positions: two are unstable and one is stable. The conditions for determining the three types of equilibrium positions are also presented. It is further found that when the two interfaces are imperfect, there always exists at least one equilibrium position for the dislocation. The results in this paper further demonstrate that the situation in which the screw dislocation interacts with two imperfect interfaces can be quite different to and more complex than the one in which a screw dislocation interacting with only one imperfect interface. We also point out that while the far-field loading solution (Eqs. (21)–(23)) can be applied to investigate the effect of the imperfect interfaces on the effective material property, the screw-dislocation solution can be extended to the study of the interaction of a crack with the two imperfect interfaces. Furthermore, since material properties of a composite can be strongly influenced by the dislocation behaviors in the material system (e.g., Leonard and Haataja, 2005), it is expected that results presented in this paper could be used as guidance for future numerical analysis of dislocation mobility and stability in multiphase systems with multiple imperfect interfaces.

Acknowledgments

The authors would like to thank the two reviewers and the editor for their constructive comments. This work was supported by AFRL 06-S531-060-C1.

References

Abe, H., Sekimura, N., Yang, Y., 2003. Stability and mobility of defect clusters in copper under displacement cascade conditions. J. Nucl. Mater. 323, 220–228.

Achenbach, J.D., Zhu, H., 1989. Effect of interfacial zone on mechanical behavior and failure of fiber-reinforced composites. J. Mech. Phys. Solids 37, 381–393.

Benveniste, Y., 2006. A general interface model for a three-dimensional curved thin anisotropic interphase between two anisotropic media. J. Mech. Phys. Solids 54, 708–734.

Benveniste, Y., Miloh, T., 1986. The effective conductivity of composite with imperfect contact at constituent interfaces. Int. J. Eng. Sci. 24, 1537–1552.

Buehler, M., Yao, H., Gao, H., Ji, B., 2006. Cracking and adhesion at small scales: atomistic and continuum studies of flaw tolerant nanostructures. Modelling Simul. Mater. Sci. Eng. 14, 799–816.

Chen, T., 2001. Thermal conduction of a circular inclusion with variable interface parameter. Int. J. Solids Struct. 38, 3081–3097.

Chen, T., Chiang, S.C., 1997. Electroelastic fields and effective moduli of a medium containing cavities or rigid inclusions of arbitrary shape under anti-plane mechanical and in-plane electric fields. Acta Mech. 121, 79–96.

Dundurs, J., 1967. On the interaction of a screw dislocation with inhomogeneities. Recent Adv. Eng. Sci. 2, 223–233.

Dundurs, J., 1970. Some properties of elastic stresses in a composite. Recent Adv. Eng. Sci. 5, 203–216.

Fan, H., Wang, G.F., 2003. Screw dislocation interacting with imperfect interface. Mech. Mater. 35, 943–953.

Freund, L.B., 2000. The mechanics of electronic materials. Int. J. Solids Struct. 37, 185–196.

Author's personal copy

Gong, S.X., Meguid, S.A., 1992. A general treatment of the elastic field of an elliptical inhomogeneity under antiplane shear. ASME J. Appl. Mech. 59, 131–135.

Gryaznov, V.G., Polonsky, I.A., Romanov, A.E., Trusov, L.I., 1991. Size effects of dislocation stability in nanocrystals. Phys. Rev. B 44, 42–46.

Hashin, Z., 1991. The spherical inclusion with imperfect interface. ASME J. Appl. Mech. 58, 444–449.

Hirth, J.P., Lothe, J., 1982. Theory of Dislocations, second ed. Wiley, New York.

Honein, T., Honein, E., Herrmann, G., 1994. Circularly cylindrical and plane layered media in antiplane elastostatics. ASME J. Appl. Mech. 61, 243–249.

Hurtado, J.A., Freund, L.B., 1999. The force on a dislocation near a weakly bonded interface. J. Elasticity 52, 167–180.

Justo, J.F., Antonelli, A., Fazzio, A., 2001. Dislocation core properties in semiconductors. Solid State Commun. 118, 651–655.

Kattis, M.A., Mavroyannis, G., 2006. Feeble interfaces in bimaterials. Acta Mech. 185, 11–29.

Lafdi, K., 2005. TEM characterization of the interface property between the fiber and matrix. Private communication.

Leonard, F., Haataja, M., 2005. Alloy destabilization by dislocations. Appl. Phys. Lett. 86, 181909-1–181909-3.

Nie, S., Basaran, C., 2005. A micromechanical model for effective elastic properties of particulate composites with imperfect interfacial bonds. Int. J. Solids Struct. 42, 4179–4191.

Pan, E., Roy, A.K., 2006. A simple plane-strain solution for functionally graded multilayered isotropic cylinders. Struct. Eng. Mech. 24, 727–740.

Penn, R.L., Banfield, J.F., 1998. Imperfect oriented attachment: dislocation generation in defect-free nanocrystals. Science 281, 969–971.

Ru, C.Q., 1999. Three-phase elliptical inclusions with internal uniform hydrostatic stresses. J. Mech. Phys. Solids 47, 259–273.

Ru, C.Q., Schiavone, P., 1997. A circular inclusion with circumferentially inhomogeneous interface in antiplane shear. Proc. R. Soc. Lond. A 453, 2551–2572.

Sudak, L.J., 2003. On the interaction between a dislocation and a circular inhomogeneity with imperfect interface in antiplane shear. Mech. Res. Commun. 30, 53–59.

Sudak, L.J., Wang, X., 2006. Green's functions in plane anisotropic bimaterials with imperfect interface. IMA J. Appl. Math. 71, 783–794.

Twu, C.J., Ho, J.R., 2003. Molecular-dynamics study of energy flow and the Kapitza conductance across an interface with imperfection formed by two dielectric thin films. Phys. Rev. B 67, 205422-1–205422-8.

Wang, X., Shen, Y.P., 2002. An edge dislocation in a three-phase composite cylinder model with a sliding interface. ASME J. Appl. Mech. 69, 527–538.

Wang, X., Zhong, Z., 2003. A circular inclusion with a nonuniform interphase layer in antiplane shear. Int. J. Solids Struct. 40, 881–897.

Xiao, Z.M., Chen, B.J., 2000. A screw dislocation interacting with a coated fiber. Mech. Mater. 32, 485–494.